NASA Technical Memorandum 83452

Application of Modern Surface Analytical Tools in the Investigation of Surface Deterioration Processes

Donald H. Buckley
Lewis Research Center
Cleveland, Ohio

Prepared for
SURTEC—KONGRESS '83
Berlin, Germany, October 24-27, 1983

NASA

APPLICATION OF MODERN SURFACE ANALYTICAL TOOLS IN THE INVESTIGATION OF SURFACE DETERIORATION PROCESSES

Donald H. Buckley
National Aeronautics and Space Administration
Lewis Research Center
Cleveland, Ohio 44135

ABSTRACT

Surface profilometry and scanning electron microscopy were utilized to study changes in the surface of polymers when eroded. X-ray photoelectron spectroscopy (XPS) and depth profile analysis indicate the corrosion of metal and ceramic surfaces and reveal the diffusion of certain species into the surface to produce a change in mechanical properties. Ion implantation, nitriding and plating and their effects on the surface are characterized. Auger spectroscopy analysis identified morphological properties of coatings applied to surfaces by sputtering.

INTRODUCTION

Events that take place on the surface of solids can have a profound effect on the mechanical behavior of the solid, chemical interactions of the solid with the environment (corrosion), role of the solid surface in initiating reactions or chemical changes (catalysis) and solid to solid interactions (tribology). It is therefore very important to characterize the solid surface as fully as is possible.

Today there are many devices and instruments that can assist in gaining a better characterization and accordingly understanding of surfaces. There include systems capable of physical, optical, mechanical and chemical identification of the surface and near surface layers.

The objective of the present paper is to indicate the use of various tools and devices in the characterization of surfaces. The subjects to be addressed include 1) material behavior; 2) environmental effects on solids; and 3) surface treatment and coatings. Each of these topic areas will be covered with examples of the usefulness of surface analysis in achieving a better fundamental understanding of events. Surfaces will be characterized physically with the surface profilometer, optically with scanning electron microscopy, mechanically with micro-hardness measurements and dislocation etch pitting and chemically with Auger emission spectroscopy and X-ray photoelectron spectroscopy analysis. Materials to be examined in surface effects on material behavior include polymers and alloys, environmental interactions with metals and ceramics and surface treatments and coatings will include ion, implantation, plating, nitriding, and sputter deposition.

TYPICAL SURFACE APPARATUS

Figure 1 is a typical apparatus chamber for surface chemical analysis. The particular system depicted in figure 1 is used for in situ friction and

wear studies when two surfaces are in solid state contact. The surface analysis capability is provided with X-ray photoelectron spectroscopy. Ion depth profiling is also available in the system for probing the subsurface chemistry of materials. The use of carousel specimen mounting permits multiple specimen analysis for corrosion, catalysis or tribological studies. The apparatus is described in greater detail in reference 1.

RESULTS AND DISCUSSION

Material Effects

Physical changes in the character of surfaces can be readily detected with the surface profilometer, a device capable of ascertaining modifications in surface topography by the use of a mechanical stylus. A typical application of such a device is in the erosion of solid surfaces. The loss of material from the surface with time can be readily followed and changes in geometry detected. Figure 2 presents surface profiles of polytetrafluoroethylene (PTFE) after erosion for various periods of time.

An examination of figure 2 indicates that bombardment of the polymer surface with glass beads at normal incidence results in material loss from the surface. The traces at various time intervals further indicate that the size of the pit continues to grow with exposure time both in area and depth.

The ordinary scanning electron microscope can be of considerable assistance in surface characterization. It has been used to follow the loss of material and changes in the surface character of polymers with erosion.

A micrograph of a polymethyl methacrylate (PMMA) surface is presented in figure 3. An erosion pit is revealed in the micrograph. The pit resulted from glass bead impingement for 15 seconds. Region 3 of figure 3(a) reveals material build up on that surface with a fissure between regions 2 and 3 ringing the pit edge (fig. 3(c)). In figure 3(b) there is evident layers or bands indicative of local melting and resolidification of the PMMA.

Figure 3 indicates that much detail about changes in surface character can be readily ascertained with the simple use of the scanning electron microscope. Thus far it can be seen that surface profile and appearance can be characterized. What about the chemical composition of the solid surface? Surface analytical tools such as X-ray photoelectron spectroscopy (XPS) are very useful for analysis of surface chemistry (refs. 3 and 4). An example of this usefulness is demonstrated with the data of figure 4.

In figure 4 the coefficient of friction for three ferrous base, amorphous alloys (metallic glasses) is plotted as a function of temperature. As the temperature increases the friction increases in the range of from 20° to 400° C. These alloys transform from the amorphous to the crystalline state at temperatures between 400° and 450° C. The increase in friction is then associated with this change in state.

At 500° C in figure 4 the friction undergoes a marked decrease from that measured at 400° C. Why does this appreciable decrease occur? Surface analysis with XPS supplies the answer to this question.

Figure 5 presents the XPS spectra for one of the ferrous base metallic glasses of figure 4 in the as received condition, after sputter cleaning, when heated to 350° and 750° C. The iron Fe_{2p}, Co_{2p}, B_{1s}, and Si_{2p} spectra as a function of binding energy are presented.

The as received surface indicates the presence of Fe_2O_3, CoO, CoB, B_2O_3, and $B(OH)_3$. Sputter cleaning removes the oxides and other surface contaminants. At 350° C SiO appears on the solid surface as indicated in figure 5(d). The cause for the reduction in friction at 500° and 750° C in figure 4 is the appearance of BN on the surface of the alloy indicated at 750° C in figure 5(c). It is also present at 500° C, is a solid lubricant and brings about the friction reduction observed in figure 4.

Environmental Effects

The corrosion of solids is intimately related to the nature of chemical reactions occurring on the solid surface. Understanding those reactions is fundamental to understanding corrosion. Making an aqueous solution even only slightly alkaline alters the surface chemistry, for example, of iron. The XPS data of figure 6 reflects this change.

In figure 6 in water Fe_2O_3 is the principal surface oxide. In a 0.01 N NaOH solution, however, the O_{1s} peak shifts indicating the formation of more complex iron compounds (ref. 5). The NaOH forms a protective film on iron which passivates the surface.

There is considerable interest currently in the mechanical use of ceramics. They, like metals and alloys, will have to function in a variety of environments including those which are corrosive. Studies are therefore being conducted on the surfaces of ceramics to determine environmental effects.

One ceramic of interest is magnesium oxide (MgO). This particular ceramic was cleaved in air and in mineral oil containing surface active agents known to affect metal surfaces. The XPS data of table I indicate the surface chemistry of the magnesium oxide cleaved in three media before and after sputter removal of surface layers. The data indicate that the chlorine containing additive interacts with the MgO surface and has penetrated into the surficial layers of the solid as chlorine is still detected on sputter removal of surface layers.

Microhardness measurements and dislocation etching of the MgO surface exposed to various environments indicates that the presence of surface active species can alter surface mechanical behavior. Figures 7 and 8 reveal these effects. The presence of sulfur in mineral oil increases the surface microhardness while chlorine decreases it as indicated in figure 7. The dislocation data of figure 8 agree with the microhardness data in that the surface concentration of dislocations, both edge and screw, is less than observed in straight mineral oil while they are greater in a chlorine environment.

The data of figures 7 and 8 are particularly interesting in that in table I no sulfur was found either on the surface or subsurface. Chlorine, however, had penetrated into the solid and can therefore explain the surface softening of figures 7 and 8.

Surface Treatment and Coatings

Ion implantation of surfaces has become a popular technique for modifying the physical and chemical behavior of surfaces. It is used with semiconductors, in providing corrosion resistance and in tribology (refs. 6 to 11).

Figure 9 is an Auger emission spectroscopy spectrum obtained from a nitrogen ion implanted steel disk surface after sputter removal of approximately 750 nm of the surface (ref. 12). The original surface had been implanted with 1.5 MeV nitrogen ions with an implantation dose of 5×10^{17} ions/cm^2. Figure 9 indicates in the Auger spectrum the presence of nitrogen subsurface confirming the implantation of nitrogen ions in the steel. The concentrations of the nitrogen ions subsurface in the steel were profiled and the results obtained are presented in figure 10.

An examination of figure 10 indicates that the maximum concentration of nitrogen resulting from implantation is not at surface (the ordinate of fig. 10), but rather at a depth of 0.8 μm subsurface. The data fit a Gaussian distribution subsurface. The data of figures 9 and 10 indicate the value of surface analysis in the study of the presence of the implanted species and in profiling its concentration within the surface layers.

In addition to ion implantation, the ions of species such as nitrogen can be utilized to modify surfaces in another manner, namely through ion nitriding. Surfaces such as steels can be treated by gaseous plasma mixtures of nitrogen with hydrogen to produce surface layers of nitride. Surface compounds can be identified in these layers (ref. 13). The nitrided surficial layers are sufficiently thick so as to permit their identification with X-ray diffractometery. The results of such an analysis are presented in figure 11.

The original steel diffractogram prior to nitriding is presented in figure 11(a). Nitriding in a nitrogen-hydrogen mixture produces the γ phase (Fe_4N), a single phase compound, indicated in figure 11(b). Adding a trace of methane (CH_4) to the plasma produces the diffractrogram of figure 11(c) which indicates the ε phase ($Fe_{2-3}N$). The Fe_4N phase of figure 11(b) forms with 5.7 to 6.1 weight percent nitrogen and has a face centered cubic structure, while the $Fe_{2-3}N$ phase forms with between 11 and 11.35 weight percent nitrogen and has a hexagonal structure.

The composition of the plasma nitrided surface can affect surface properties such as tribological behavior as indicated in figure 12. Coefficient of friction is plotted in figure 12 as a function of the number of repeated cyles over the same surface (ref. 13).

Nitriding reduces friction in figure 12. Further, there are friction differences between the γ and ε phases. In addition ion treating both surfaces (rider and substrate of fig. 12) produces even lower friction.

Yet another ion technique for application to surfaces is that of ion plating, where a very thin metallic layer is deposited on and buried in the surface layers. A coating results which can provide corrosion or tribological protection or be used as a catalytic surface. The advantage of ion plating over other techniques for the application of this protective film is that a diffuse graded interface is produced from the kinetic energy associated with the depositing metallic ions. This results in a very tenacious coating.

Because the unique features of ion plating reside in its ability to develop the diffuse or graded interface it is very important to be able to characterize the interfacial region. Surface analysis with XPS and with depth profile characterization can provide insight into the region between coating and the substrate. Figures 13 and 14 present depth profile analysis with XPS for gold deposited on two different substrates nickel and iron.

Figure 13 indicates a very broad or diffuse interface between the gold coating and the nickel substrate. This is believed to be due to the solid solubility of gold in nickel (ref. 14). In contrast, the interface between gold and iron in figure 13 is much sharper. The gold on the iron is only atomically dispersed in the iron and thus a physically bonded interface is found. With the nickel, however, it is true interfacial alloying with the gold.

Surface analytical techniques can also be very useful in studying the morphology of coatings applied to surfaces by other techniques such as sputter deposition. Molybdenum disulfide (MoS_2) is a compound applied to surfaces by sputter deposition for tribological applications. The material possess a hexagonal close packed layer lattice structure. Sometimes immediately upon sputter deposition the coating was found to lack lubricating properties. With rubbing or wiping of the film the coatings became good lubricants. This effect was traced to a reorientation of the MoS_2 platelets with rubbing or wiping as indicated in figure 15 (ref. 15).

Auger emission spectroscopy analysis of the surface immediately after sputter deposition and then with wiping presented different spectra. These are presented in figure 16. The two largest peaks in both spectra are for sulfur and carbon. Sulfur is the largest. Note that the intensity ratios of carbon to sulfur change with reorientation of the MoS_2 platelets on the surface. In the as sputtered state a greater amount of sulfur relative to carbon is exposed than is after wiping. The wiping reorients the basal planes increasing the amount of carbon detected.

CONCLUSIONS

The analysis of surfaces can provide considerable insight into the behavior of materials. Techniques which have proven effective involve physical, optical and chemical principles. They have provided the following:

(1) Detail profiles of eroded surfaces by the use of the physical technique of surface profilometery.

(2) Changes in polymer surface morphology using scanning electron microscopy.

(3) Chemical surface changes due to segregation from bulk metallic glasses using XPS analysis.

(4) Identification of corrosive attack of metals and ceramics by environmental constituents using XPS and depth profile analysis.

(5) Ion effects upon surfaces associated with implantation, gaseous reactions and plating using Auger, XPS, depth profiling and conventional X-ray techniques to characterize the surface and near surface regions.

(6) Morphological changes in sputter deposited films with mechanical surface activity revealed by Auger emission spectroscopy analysis.

REFERENCES

1. Miyoshi, K; and Buckley, D. H.: XPS, AES, and Friction Studies of Single-Crystal Silicon Carbide. Appl. Surf. Sci., vol. 10, no. 3, 1982, pp. 357-376.
2. Rao, P. V.; and Buckley, D. H.: Spherical Micro-Glass Particle Impingement Studies of Thermoplastic Materials at Normal Incidence. NASA TM-83410, 1983.
3. Buckley, D. H.: Surface Effects in Adhesion, Friction, Wear and Lubrication. Elsevier (Amsterdam), 1981.
4. Miyoshi, K.; and Buckley, D. H.: Friction and Wear of Some Ferrous-Base Metallic Glasses. NASA TM-83067, 1983.
5. Rengstorff, G. W. P.; Miyoshi, K.; and Buckley, D.: Friction and Wear of Iron and Nickel in Sodium Hydroxide Solutions. NASA TM-82935, 1982.
6. Townsend, P. D.; Kelly, J. C.; and Hartley, N. E. W.: Ion Implantation, Sputtering and their Applications. Academic Press (London), 1976.
7. Mayer, J. W.; Eriksson, L.; and Davies, J. A.: Ion Implantation in Semiconductors, Silicon and Germanium. Academic Press, 1970.
8. Ashworth, V., et al.: Effect of Ion Implantation on the Corrosion Behavior of Iron. Ion Implantation in Semiconductors; Science and Technology, S. Namba, ed., Plenum Press, 1975, pp. 367-373.
9. Khirnyi, Yu. M.; and Solodovnikov, A. P.: Effect of Increased Corrosion Resistance in Metals Irradiated with Helium Ions. Sov. Phys. Dokl., vol. 19, no. 1, July 1974.
10. Hartley, N. E. W.: Tribological Effects in Ion-Implanted Metals. Applications of Ion Beams to Materials, Inst. Phys. Conf. 28, G. Carter, W. A. Grant, and J. S. Colligan, eds., 1976, pp. 210-223.
11. Jones, W. R., Jr., and Ferrante, J.: The Effect of Nitrogen Ion (N^+) Implantation on the Friction and Wear Characteristics of Iron. NASA TM-79029, Nov. 1978.
12. Ferrante, J.; and Jones, W. R., Jr.: Friction Wear and Auger Analysis of Iron Implanted with 1.5-MeV Nitrogen Ions. NASA TP-1989, Mar. 1982.
13. Spalvins, T.: Tribological and Microstructural Characteristics of Ion-Nitrided Steels. NASA TM-83368, 1983.
14. Miyoshi, K.; Spalvins, T.; and Buckley, D. H.: Tribological Properties and X-ray Photoelectron Spectroscopy Studies of Ion-Plated Gold on Nickel and Iron. Thin Solid Films, vol. 96, 1982, pp. 9-16.
15. Spalvins, T.: Morphological and Frictional Behavior of Sputtered MoS_2 Films. NASA TM-82809, 1982.

TABLE I. - RELATIVE CONCENTRATION OF CONSTITUENTS IN MgO SURFICIAL LAYER BEFORE AND AFTER SPUTTERING

Surface treatment before installation in vacuum chamber	Surface treatment in vacuum chamber	Concentration				
		Mg	O	C	Cl	S
Cleaved in air	No treatment	0.44	0.51	0.05	----	----
	Sputtering	.47	.53	----	----	----
Cleaved in mineral oil containing chlorine additive	No treatment	.32	.30	.36	0.02	----
	Sputtering	.51	.48	Negligible	.01	----
Cleaved in mineral oil containing sulfur additive	No treatment	.36	.31	.33	----	----
	Sputtering	.52	.48	Negligible	----	----

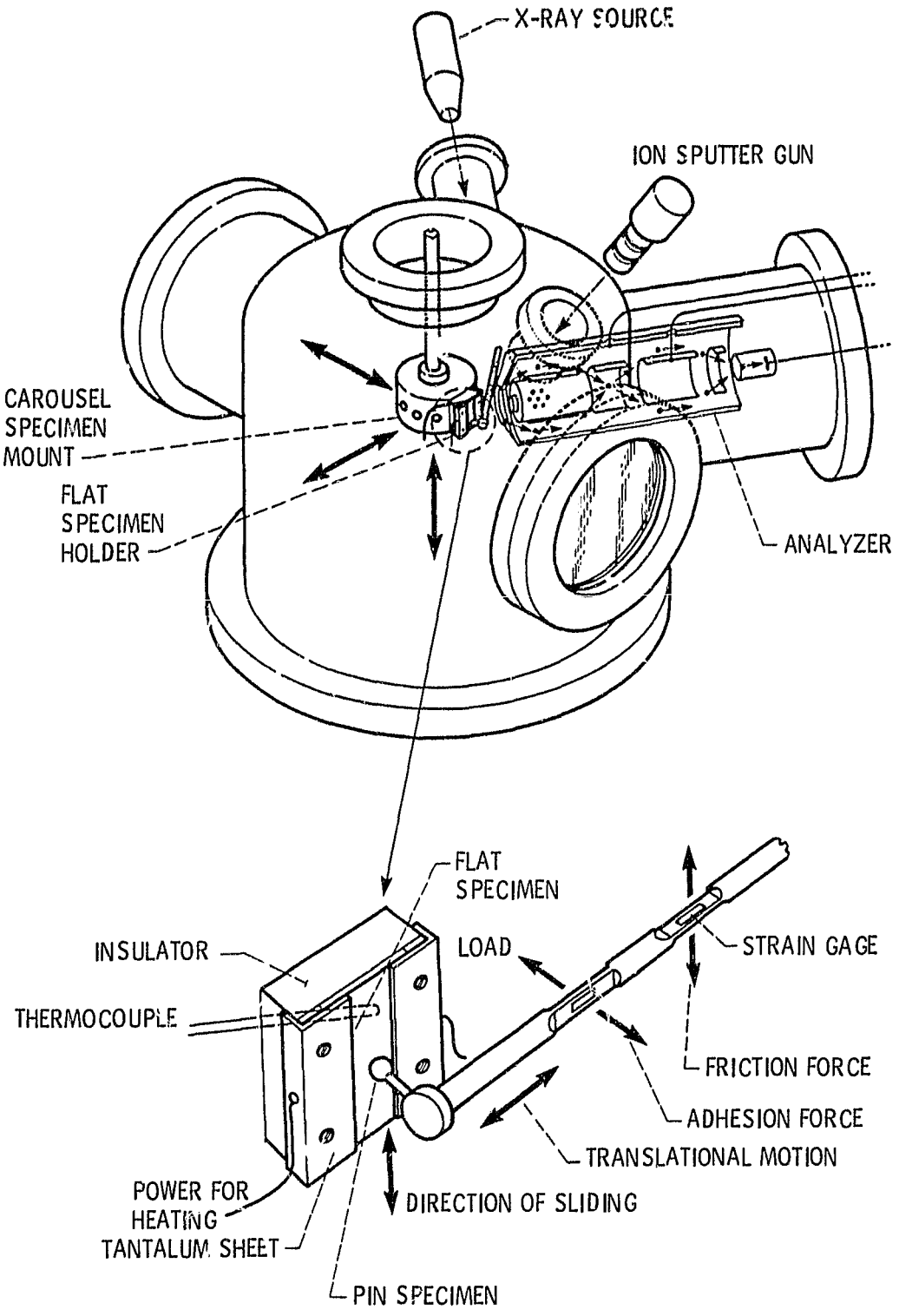

Figure 1. - Friction and wear apparatus.

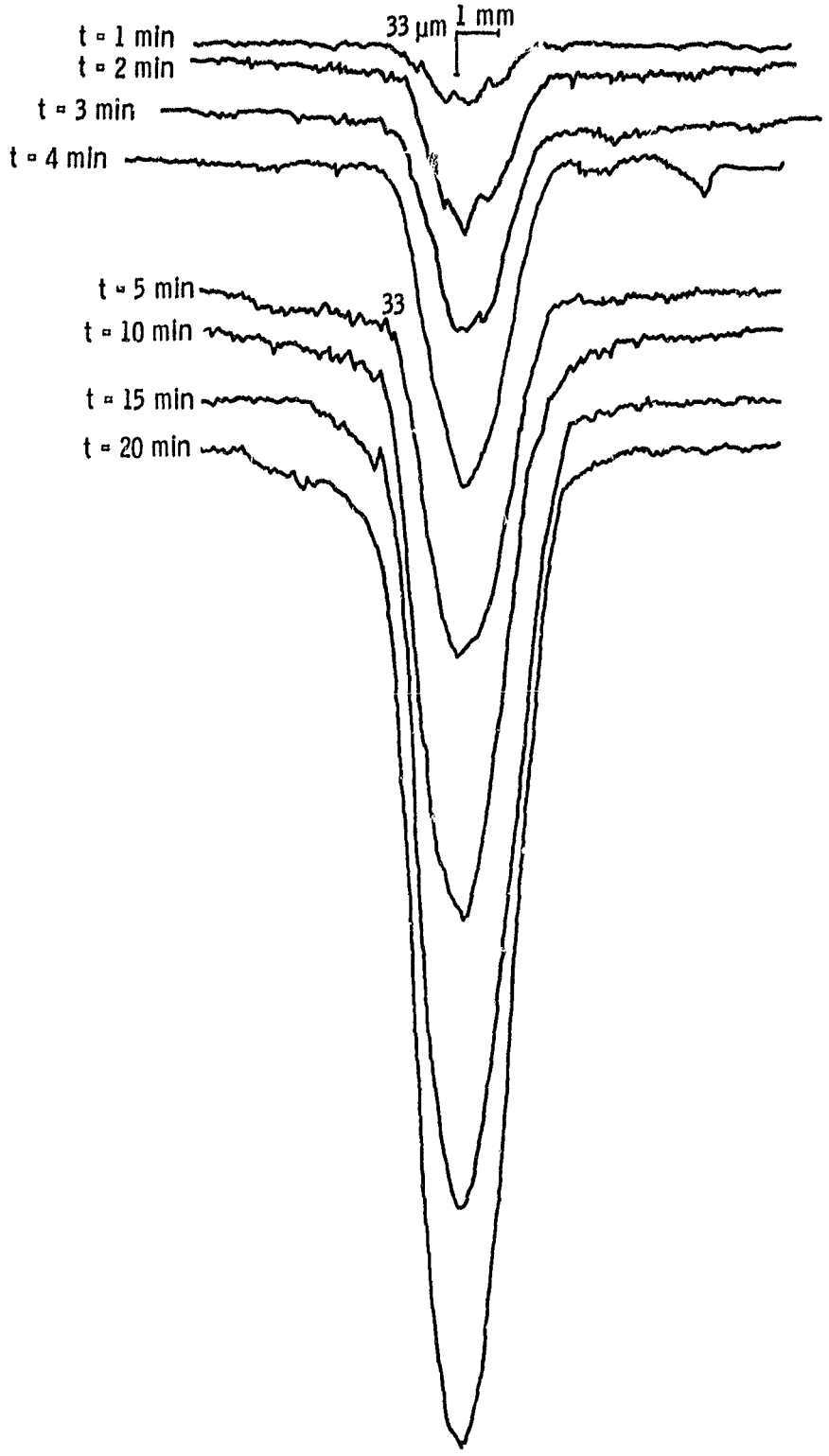

Figure 2. - Surface traces on PTFE as a function of erosion time.

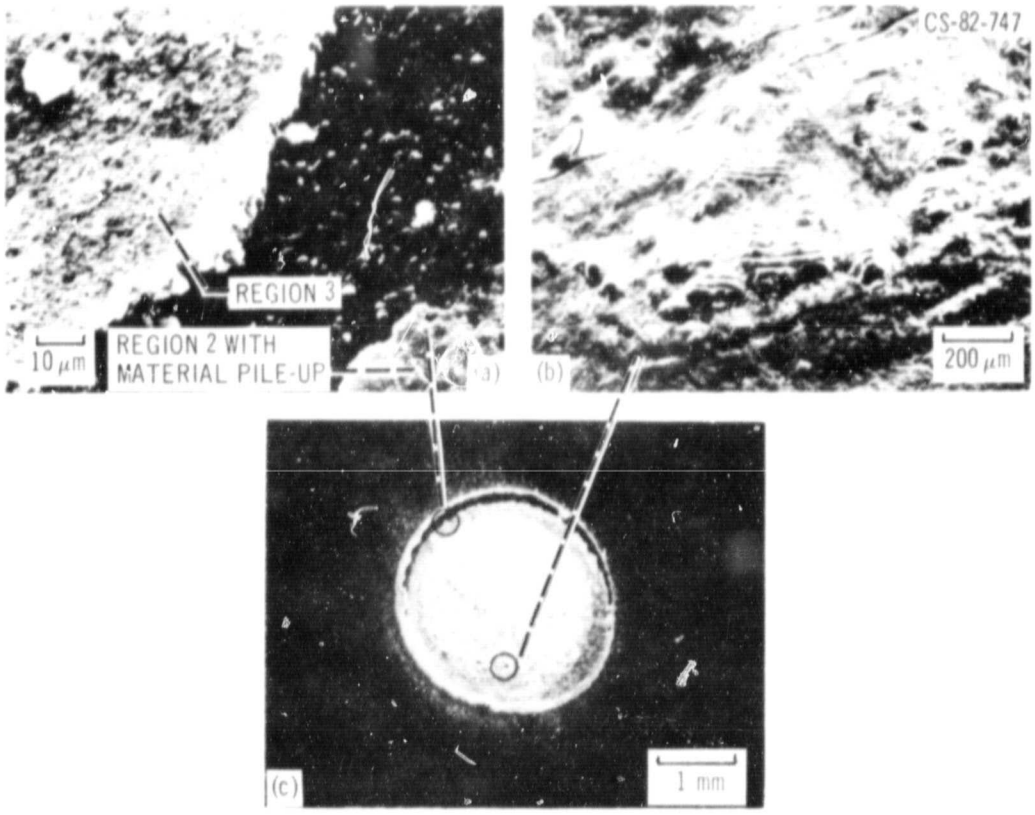

(a) Details of regions 2 and 3.

(b) Material buildup with possible stratification.

(c) Micrograph of material flow of an eroding pit.

Figure 3. - SEM micrographs (40° tilt) of PMMA specimen surface exposed to glass bead impingement. Time, 15 secs; gas pressure, 0.27 MPa. Particle velocity, 72 m/s.

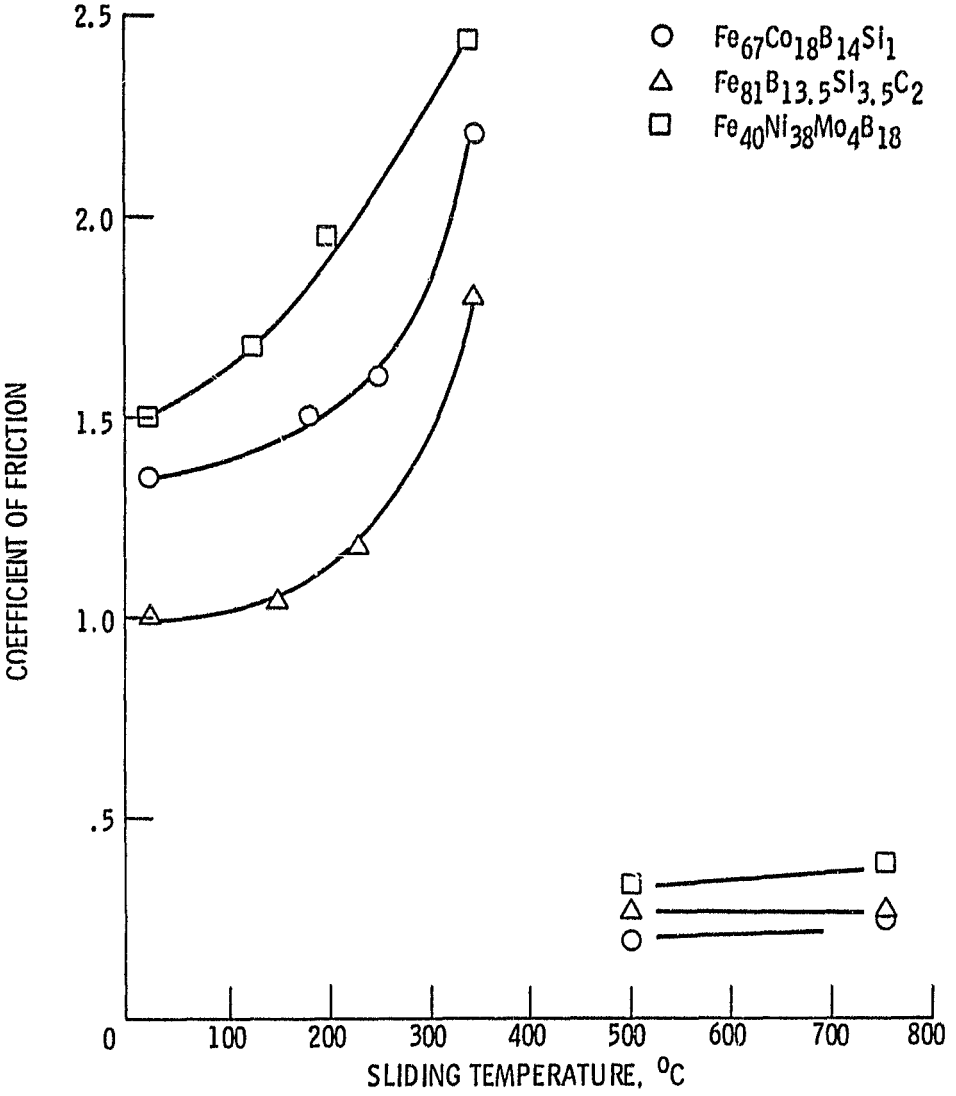

Figure 4. - Coefficient of friction as a function of temperature for aluminum oxide sliding on $Fe_{67}Co_{18}B_{14}Si_1$, $Fe_{81}B_{13.5}Si_{3.5}C_2$, and $Fe_{40}Ni_{38}Mo_4B_{18}$ in vacuum. Normal load, 0.2 N; sliding velocity, 3 mm min; vacuum, 10 nPa.

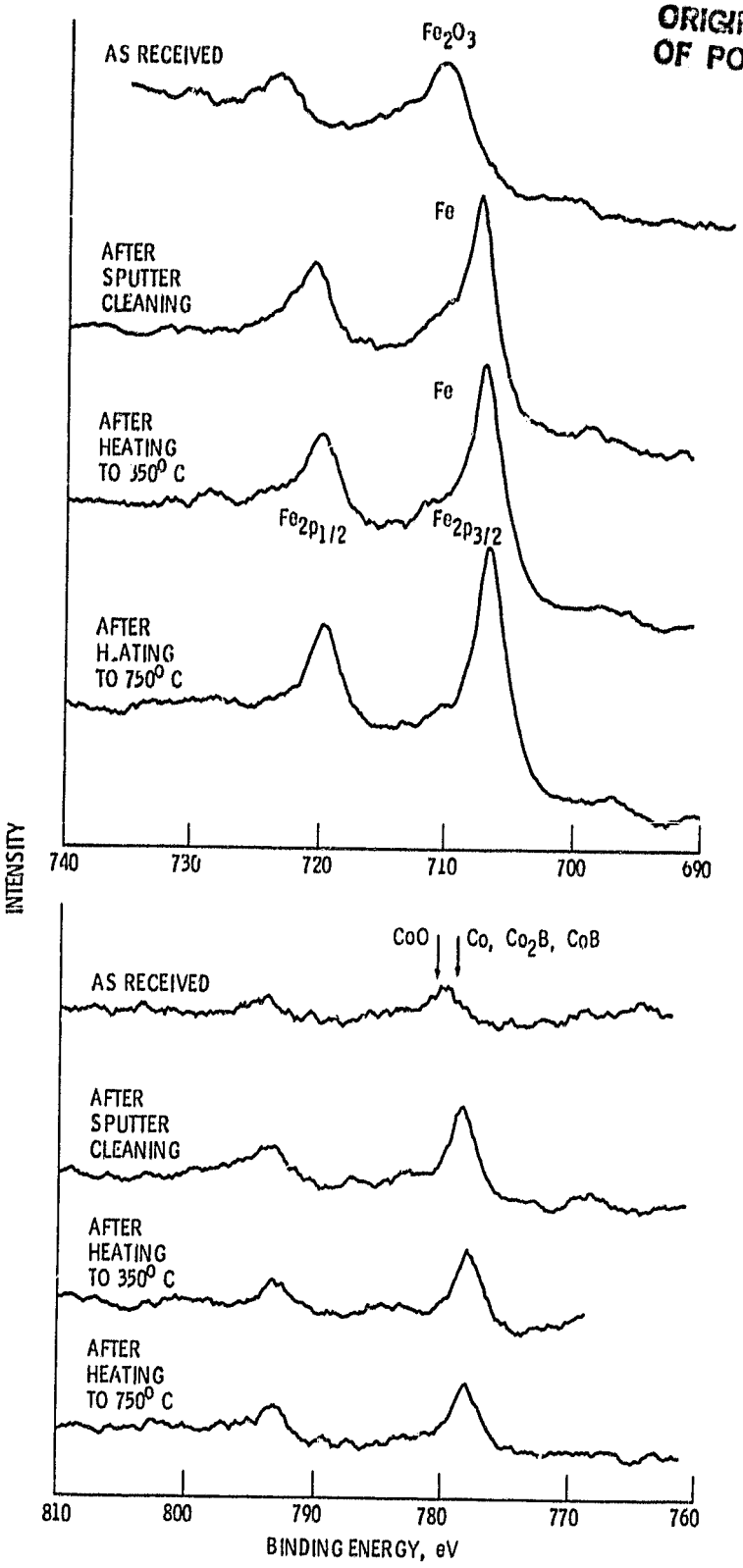

(a) Fe_{2p}.
(b) Co_{2p}.

Figure 5. - Representative Fe_{2p}, Co_{2p}, B_{1s}, Si_{2p}, and C_{1s} XPS peaks on $Fe_{67}Co_{18}B_{14}Si_1$ surface.

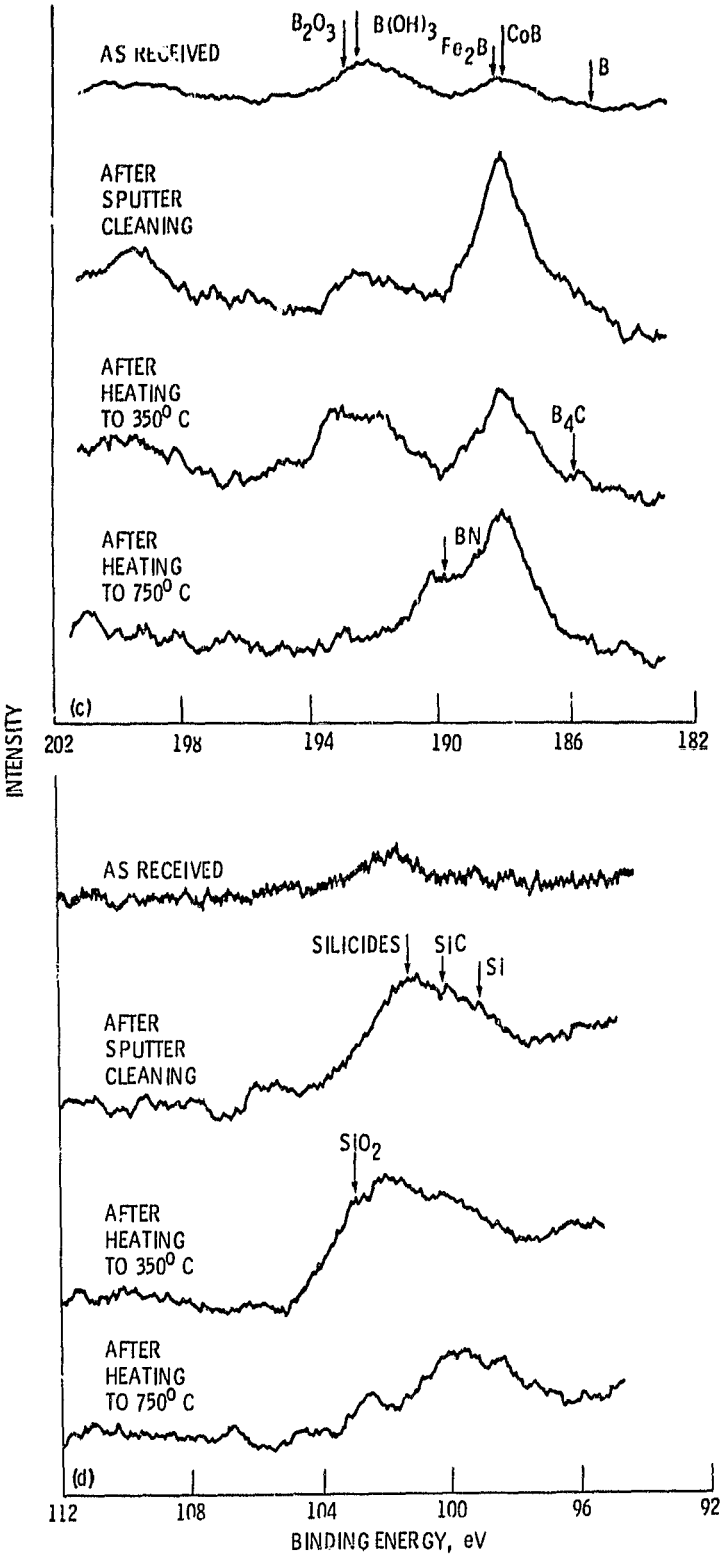

(c) B_{1s}.
(d) Si_{2p}.

Figure 5. - Concluded.

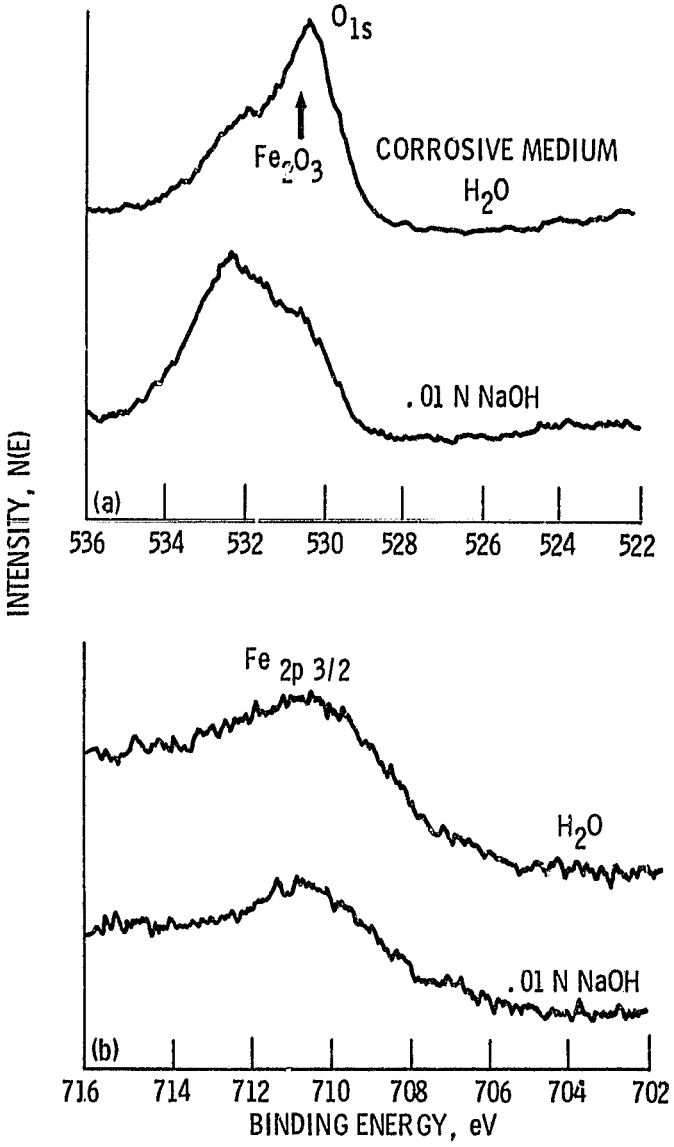

Figure 6. - XPS data on surface of iron.

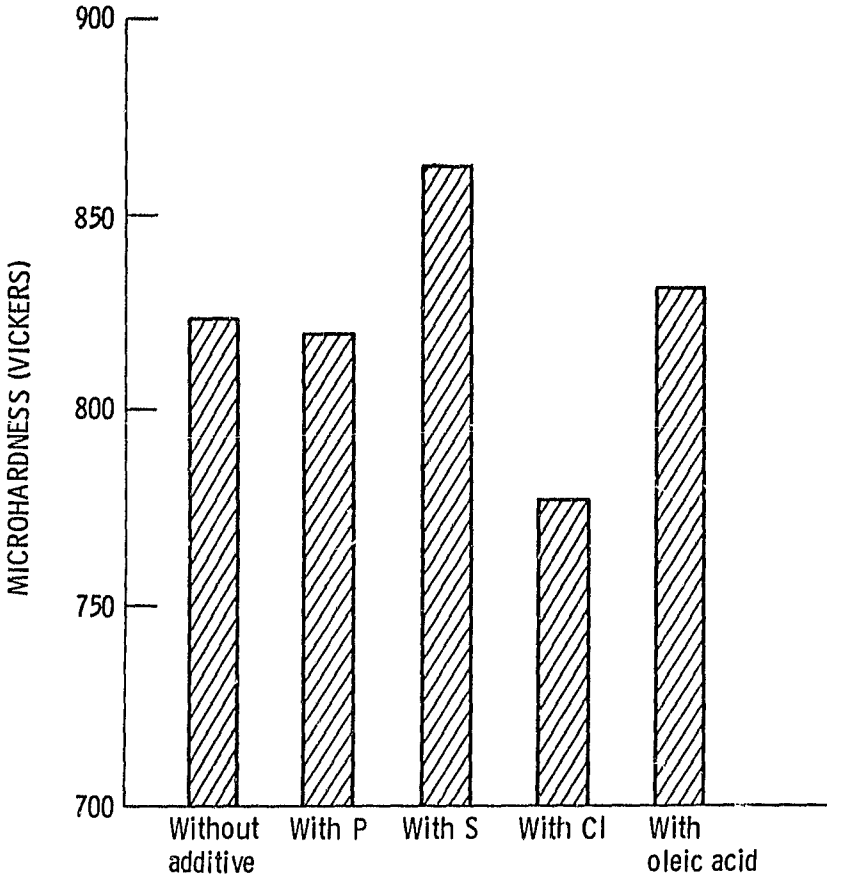

Figure 7. - Microhardness (Vickers) of magnesium oxide (001) surface cleaved and hardness measurements conducted) in mineral oil with and without various additives. Additives containing phosphorus, sulfur, chlorine, or oleic acid; load, 0.1 N; indenter, diamond; room temperature.

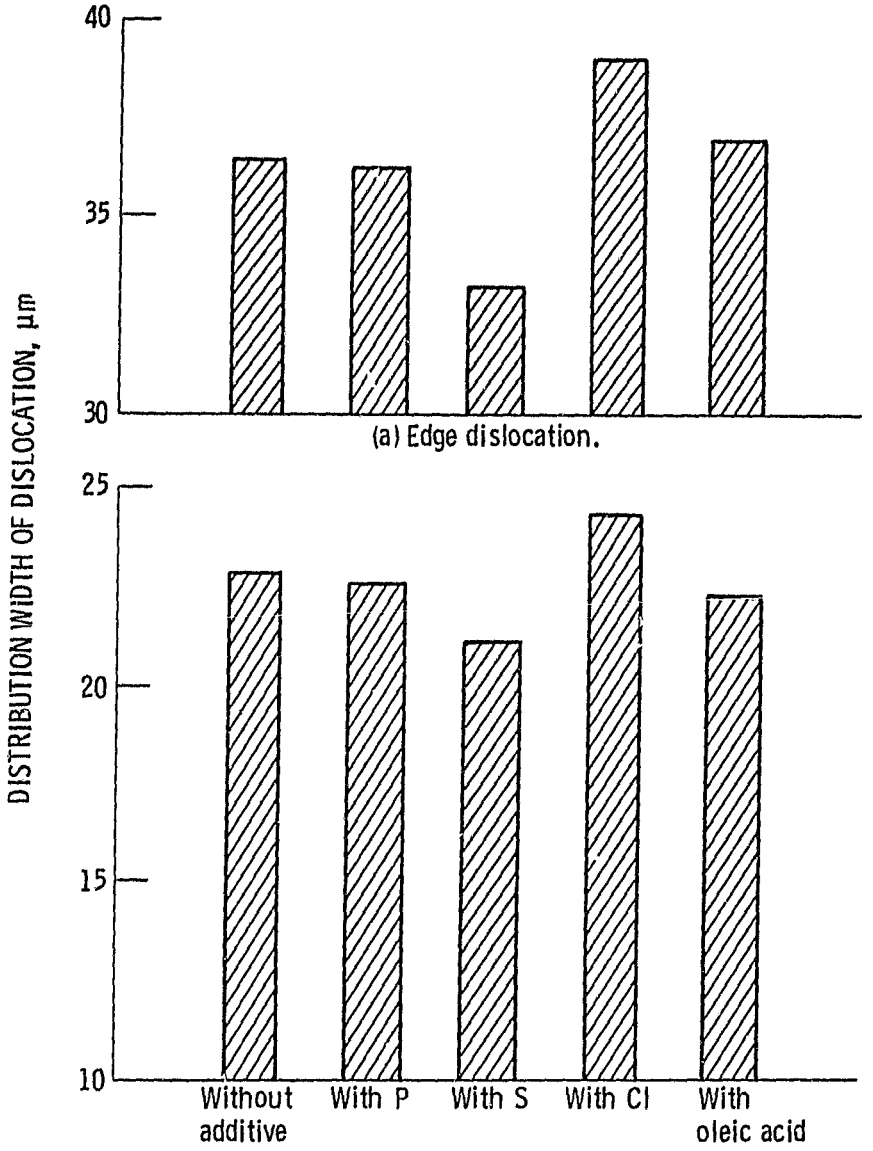

(a) Edge dislocation.

(b) Screw dislocation.

Figure 8. - Distribution widths of edge and screw dislocations around Vickers indentations on cleaved magnesium oxide {001} surface. Indentations were conducted in mineral oil with and without various additives. Additives containing phosphorous, sulfur, chlorine, or oleic acid; load, 0.1 N; indenter, diamond; room temperature.

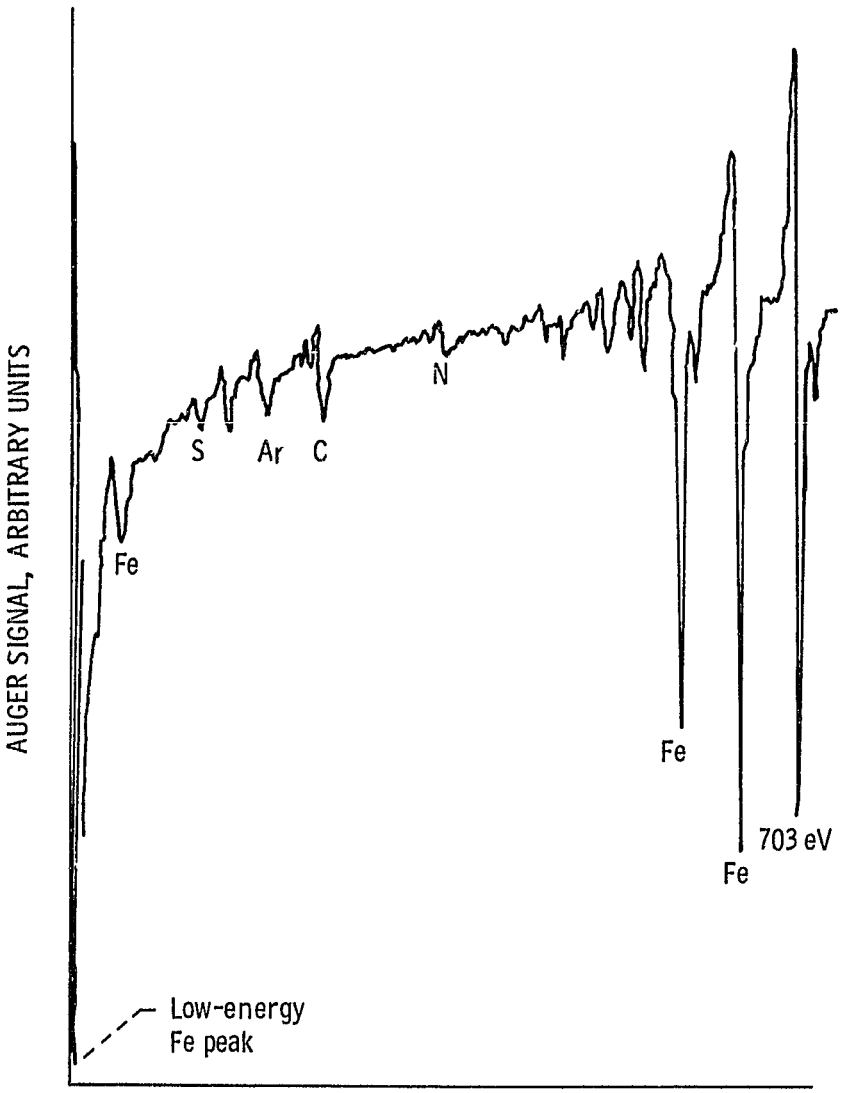

Figure 9. - Auger spectrum of nitrogen-implanted steel disk surface after 660 minutes of sputtering (~750 nm).

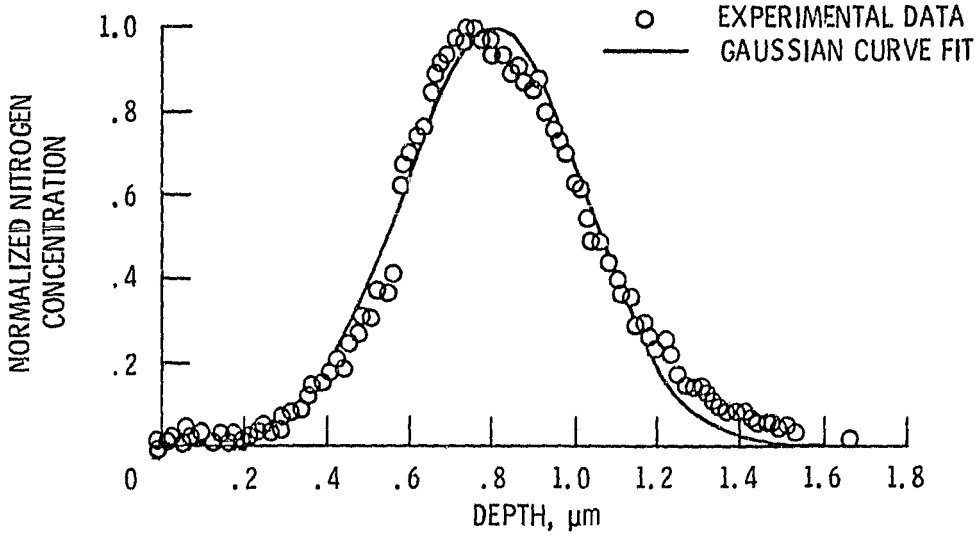

Figure 10. - Nitrogen concentration as a function of depth in nitrogen-implanted steel disk.

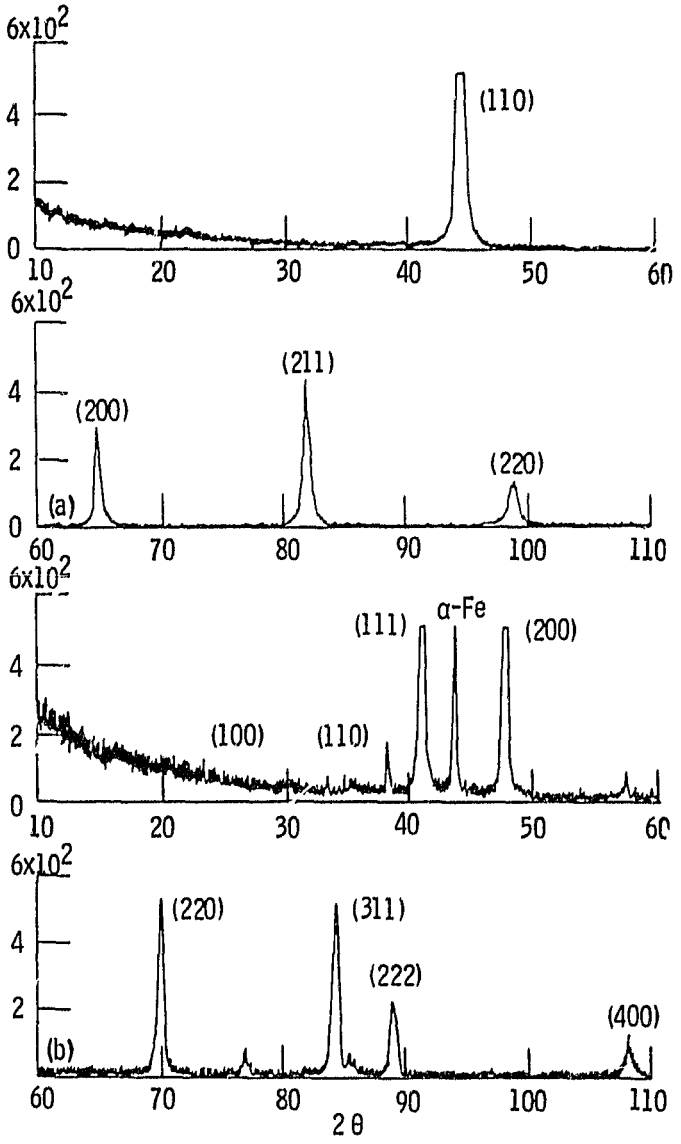

(a) Original AISI 4140 steel.
(b) Ion nitrided in 75% H_2-25% N_2.

Figure 11. - X-ray diffractograms of ion nitrided AISI 4140 steel.

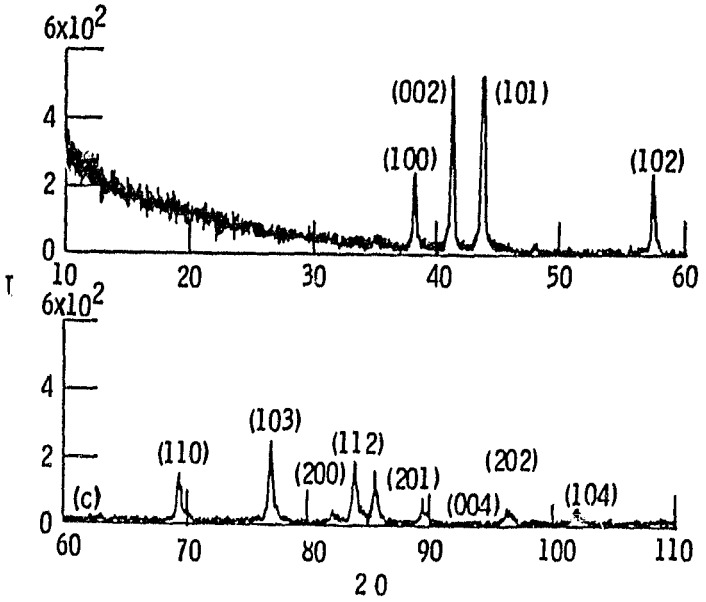

(c) Ion nitrided in 75% H_2-25% N_2+trace CH_4.

Figure 11. - Concluded.

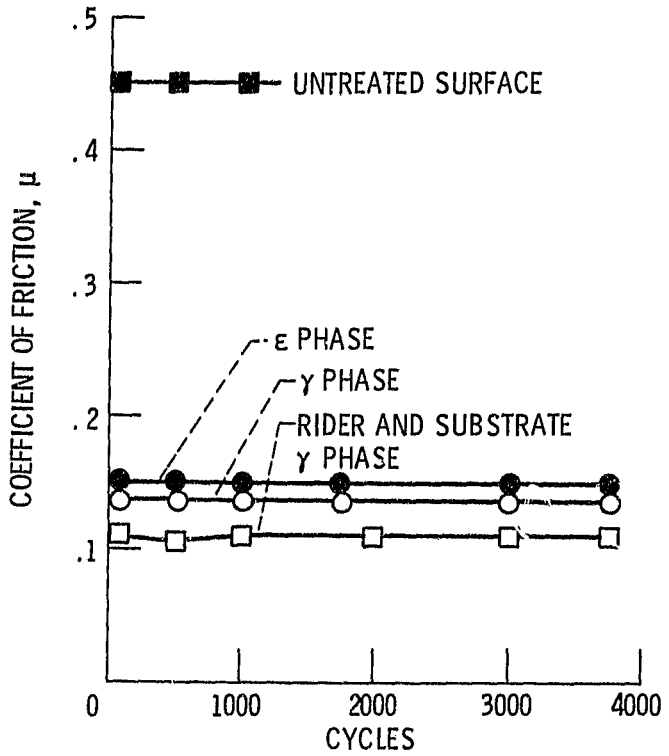

Figure 12. - Comparison of the coefficients of friction of ion nitrided 4140 steel surfaces (440 C rider; load, 250 GF; speed, 1.52 $Mmin^{-1}$; pressure, 2×10^{-3} torr).

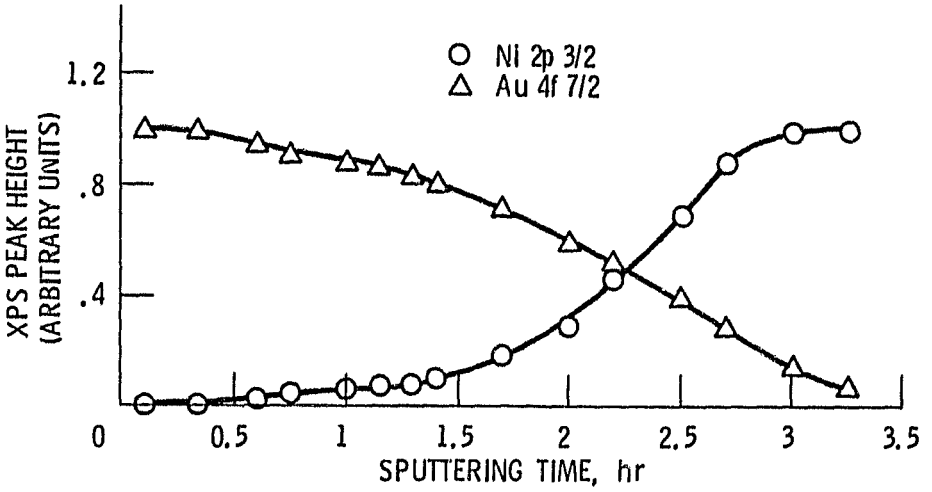

Figure 13. - Elemental depth profile of the ion plated gold on nickel. Thickness of gold film on nickel, 0.6 micrometer.

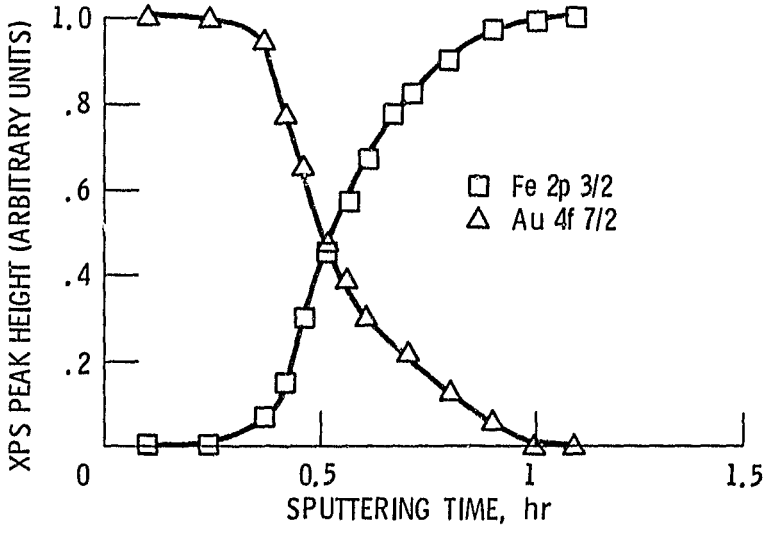

Figure 14. - Elemental depth profile of the ion plated gold on iron. Thickness of gold film on nickel, 0.6 micrometer.

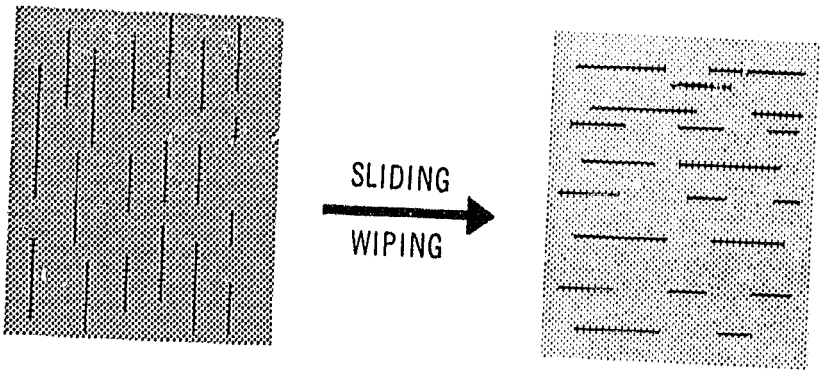

Figure 15. - Reorientation of sputtered MoS_2 platelets.

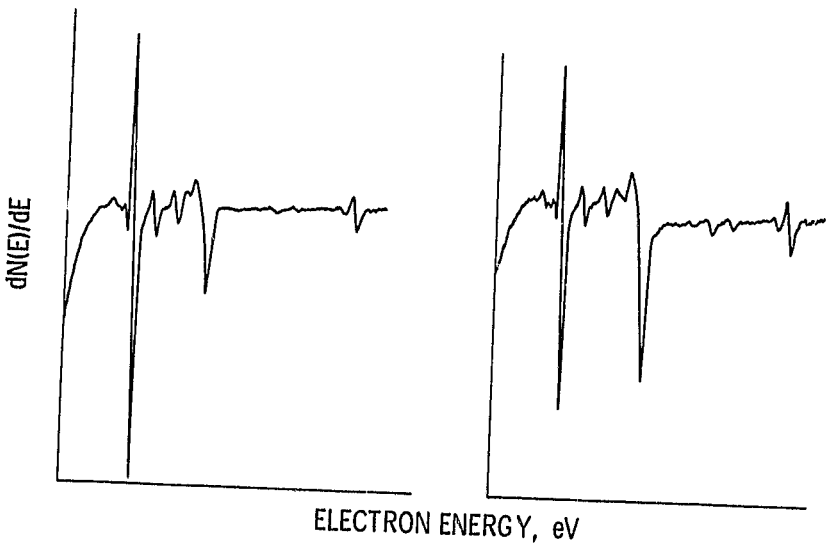

(a) As sputtered. (b) After wiping.

Figure 16. - Auger spectra of sputtered MoS_2 films.